environmental sciences proceedings

MDPI

Proceeding Paper

Verification of the Short-Term Forecast of the Wind Speed for the Gibara II Wind Farm according to the Prevailing Synoptic Situation Types †

Dayanis María Patiño Avila [1,*], Alfredo Roque Rodríguez [1], Edgardo Soler Torres [2], Arlén Sánchez Rodríguez [3], Thalía Gómez Lino [3] and Rosalba Olivera Bolaños [3]

[1] Atmospheric Physics Center, Institute of Meteorology, Havana 11700, Cuba; alfroquerodriguez@gmail.com
[2] Meteorological Center, Island of Youth, Havana 11700, Cuba; edgardo.soler2@gmail.com
[3] Higher Institute of Technologies and Applied Sciences, Havana 11700, Cuba; arlensr25112001@gmail.com (A.S.R.); thaliagomezlino@gmail.com (T.G.L.); rosalbaoliverabolanos@gmail.com (R.O.B.)
* Correspondence: dayanmario212@gmail.com
† Presented at the 6th International Electronic Conference on Atmospheric Sciences, 15–30 October 2023; Available online: https://ecas2023.sciforum.net/.

Abstract: In Cuba, short-term predictions have been developed for wind speed in the Gibara wind farms. These predictions present an mean absolute error (MAE) that sometimes exceeds 3 m/s. This study aims to verify the wind forecast generated by SisPI using the Synoptic Situation Types Catalog (TSS), a form of wind speed observation data provided by the anemometers installed in the wind turbine. The study period spanned from May 2020 to April 2021. For the evaluation, the metrics root mean square error (RMSE) and MAE were used, and the analysis was made in the rainy and dry seasons via the methodology developed by Patiño (2023). The results indicate that subtype 3 (extended undisturbed anticyclonic flow) had the highest frequency of cases between very good and good in both seasonal periods. Subtype 19 (migratory anticyclone in an advanced state of transformation) was the system that produced the worst results in the dry season, with the largest number of cases of bad wind speed forecasts. The results of the statistical bias (BIAS) and Pearson's Correlation Coefficient (R) were very favorable.

Keywords: wind energy; short-term forecast; wind speed; types of synoptic situations

Citation: Avila, D.M.P.; Rodríguez, A.R.; Torres, E.S.; Rodríguez, A.S.; Lino, T.G.; Bolaños, R.O. Verification of the Short-Term Forecast of the Wind Speed for the Gibara II Wind Farm according to the Prevailing Synoptic Situation Types. *Environ. Sci. Proc.* **2023**, *27*, 25. https://doi.org/10.3390/ecas2023-15160

Academic Editor: P.W. Chan

Published: 19 October 2023

1. Introduction

Wind energy is a renewable source that harnesses the power of the wind to generate electricity. However, from an energy perspective, wind exhibits significant variations in both time and space. These variations can be quite pronounced even over short periods, meaning that wind energy generation can be intermittent and subject to large changes in short spans. This, in turn, suggests that accurately predicting the amount of energy that wind farms will generate can be a challenging task.

Unlike other power plants, which can adjust their production according to demand, wind farms are at a disadvantage due to their intermittent nature. This situation has led to the need for developing wind forecasting models that allow for a more accurate prediction of the amount of energy that will be generated at any given time. In this way, the aim is to minimize the impact of wind variability on the operation of wind farms and ensure a constant supply of electricity.

According to the most recent report from the Global Wind Energy Council [1] (77.6 GW of wind power capacity was added to electrical grids in 2022. This resulted in a 9% increase in the total installed wind power capacity, which now stands at 906 GW compared to the previous year, 2021.

Cuba, for its part, has four experimental wind farm installations with a total capacity of 11.8 MW. Out of these, the ones installed in northern Holguín, Gibara I and II (9.6 MW), have achieved an annual capacity factor exceeding 27% [2].

Accurate wind speed forecasts are essential due to the significant economic investments made in the Gibara region. These forecasts play a crucial role in predicting the amount of energy generated by wind farms, which is vital for the daily planning of the National Load Dispatch (DNC).

Currently, short-term forecasts for wind energy production are widely used internationally. One of the most relevant projects in this field is ANEMOS [3], whose main objective was to develop advanced prediction models that improve upon existing tools. Additionally, there are other important works in this area, such as those conducted by [4–11].

In Cuba, studies have been conducted to predict short-term wind in wind farms, as in the case of [12–18], where it was found that improving the resolution of the SisPI model (WRF) to 1 km yielded better results compared to previous studies. However, there were days when the forecast was not accurate, with errors exceeding 4 m/s at a resolution of 3 km. In order to understand the causes of this behavior, a study was carried out by [19]. In this work, wind speed forecasts based on MAE were analyzed in relation to TSS as the main wind-generating factor in Cuba. The study was conducted in the Gibara I Wind Farm during the period from May 2020 to April 2021.

To expand on the previous research, it was decided to extend the study to the Gibara II Wind Farm, using additional metrics to gain a more comprehensive understanding of the forecasts, considering that one of the possible factors influencing accurate forecasts is the behavior of synoptic-scale winds, which may not be well represented by the forecast model, and therefore, the results may not be as expected.

2. Materials and Methods

The Gibara I and Gibara II wind farms are located in the province of Holguin, near the coastline, about 300 m away, and have an elevation of 3 m above sea level. The Gibara II Wind Farm (PEGII), manufactured by GOLDWIND, has a capacity of 4.5 MW and has six wind turbines (Figure 1).

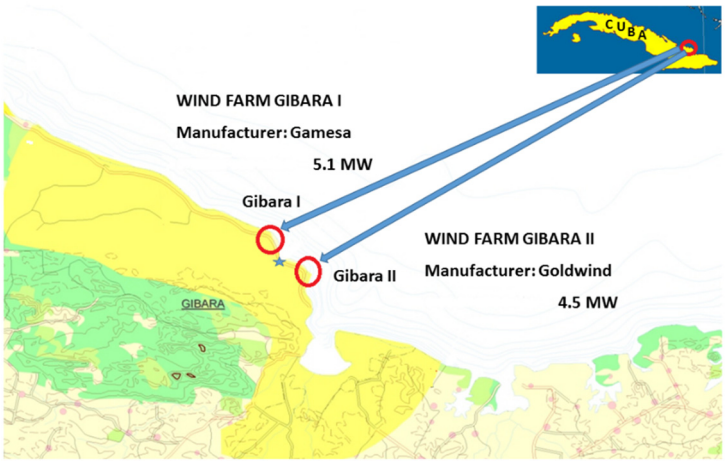

Figure 1. Location of the Gibara I and II wind parks in the Holguin province. The circles represent the wind parks in Gibara. The star between both parks represents Los Cocos wind survey mast. Note: Taken from [18].

2.1. Data Used

The research period spanned from 1 May 2020 to 30 April 2021. During this period, the Gibara II Wind Farm (PEGII) had 6 wind turbines in operation.

Hourly wind speed values from anemometers located on the nacelles of the wind turbines at a height of 55 m were used. Hourly wind speed forecast values were provided

by the Immediate Forecast System (SisPI), which uses the Weather Research and Forecasting (WRF) atmospheric model.

The Synoptic Situation Subtypes (subTSS) database was provided by [20], as well as the Catalogue of Synoptic Situation Types, where they are characterized. However, in this study, we used the thirteen subtypes that were observed daily in Gibara during the 2020–2021 research period, which are included in the [19] study and are shown in Table 1 and Figure 2.

Table 1. Synoptic Situation Subtypes presented in Gibara. Note: Taken from [19].

No	SubTSS
1	Subtropical anticyclone with first quadrant flow
2	Subtropical anticyclone with second quadrant flow
3	Extended undisturbed anticyclonic flow
4	Extended flow in the divergent sector of waves
5	Weak barometric gradient
6	Influence of a tropical cyclone
7	East waves and troughs
8	West convergence and troughs
13	Classic cold front
14	Reverse cold front
17	Migratory continental anticyclone
18	Migratory anticyclone in the process of transformation
19	Migratory anticyclone in an advanced stage of transformation

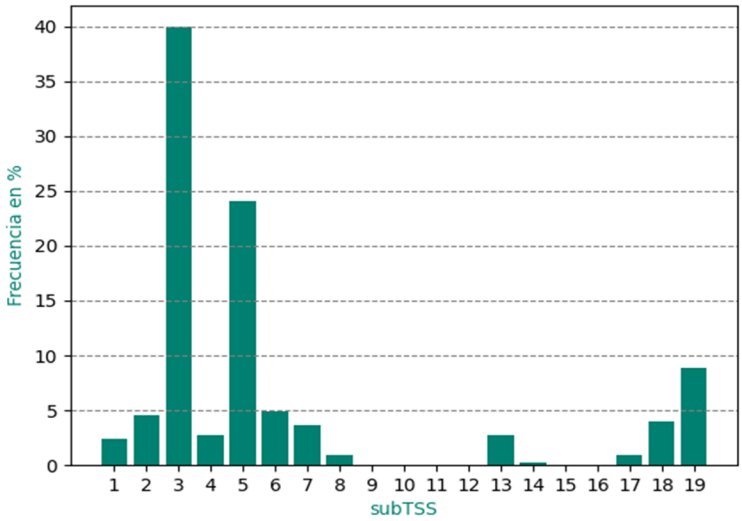

Figure 2. Annual behavior of the subTSS in the study period (May 2020 to April 2021). Note: Taken from [19].

2.2. Immediate Forecast System (SisPI)

Wind speed forecast data were generated by SisPI, a system that predicts short-term weather phenomena. This system has a forecast range of 24 h, with four daily updates every six hours (0000, 0600, 1200, and 1800 UTC) and three domains with resolutions of 27, 9, and 3 km. SisPI is initialized with data from the Global Forecast System (GFS) and uses the Weather Research and Forecasting (WRF) atmospheric model, which is widely used in wind resource research around the world [21].

2.3. Used Metrics

The metrics used were Mean Absolute Error (MAE) (1); Root Mean Square Error (RMSE) (2); Bias (BIAS) (3); and Pearson correlation coefficient (R) (4).

$$MAE = \frac{1}{n}\sum_{i-1}^{n}|\hat{x}_i - x_i| \quad (1)$$

$$RMSE = \frac{1}{n}\sum_{i-1}^{n}(\hat{x}_i - x_i)^2 \quad (2)$$

$$BIAS = \frac{1}{n}\sum_{i-1}^{n}(\hat{x}_i - x_i) \quad (3)$$

$$R = \frac{\sum(x_i - \overline{x_i})(y_i - \overline{y_i})}{\sqrt{\sum(x_i - \overline{x_i})^2(y_i - \overline{y_i})^2}} \quad (4)$$

where $\hat{x}_i$ is the observed value, and x_i is the forecast value at time i.

2.4. Methodology

Based on the subtypes that occurred in Gibara during the research period conducted by [19], the same methodology used by the author was applied. Firstly, the daily variation in wind speed for the specific area was studied. Subsequently, the Mean Absolute Error (MAE) and the Root Mean Square Error (RMSE) of the wind speed forecast in Gibara II were determined, and their behavior with respect to the subtype was analyzed. In this way, the MAE and RMSE could be classified as very good if the values were between 0 and 1 m/s; good between 1 and 2 m/s; fair between 2 and 3 m/s; and poor when the values were greater than 3 m/s. The values classified as fair and poor with respect to the subTSS were analyzed in the two seasonal periods (PLL and PPLL) to determine if there was any relationship between them. Finally, unlike Gibara I, the BIAS and R statisticians were analyzed in this research.

3. Discussion of Results

3.1. Analysis of Wind Speed Behavior in Gibara during the Period from May 2020 to April 2021

Figure 3 shows that wind speed in Gibara decreases during the early hours of the morning until 7:00 a.m. local time, similar to Gibara I in the previous study conducted by [19]. This behavior was pointed out by [22–24]. These authors explain that this decrease is due to the interaction between the predominant synoptic flow and the local circulation of sea breezes on the north coast. Starting at 7:00 a.m. local time, wind speed begins to increase and reaches its maximum value at 3:00 p.m. local time, but after 5:00 p.m. local time, it decreases again.

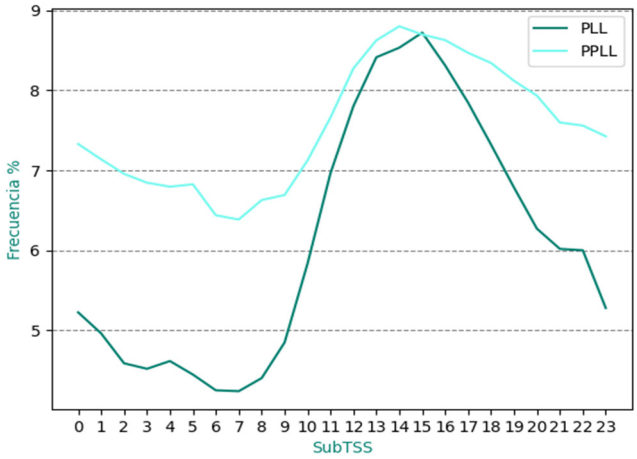

Figure 3. Daily wind speed behavior in PEGII during the period (May 2020 to April 2021).

In addition, the figure also shows that the highest values of wind speed occur during the characteristic period of the passage of frontal systems and the presence of the Migratory Continental Anticyclones, which was reported by [25]. Despite these differences, the average maximum values occur at the same times in both analyzed periods.

3.2. Forecast Behavior of Wind Speed in the Period from May 2020 to April 2021 via MAE Analysis

Figure 4 shows that the forecasts of the studied cases were classified as very good in 10.4% of the cases; good in 53% of the cases; regular in 26.8% of the cases; and 9.8% of the cases were classified as bad.

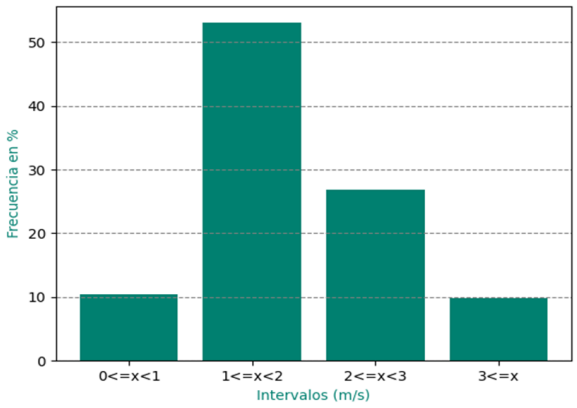

Figure 4. Frequency of the MAE statistic in 4 defined intervals for PEGII.

In more detail, more than 60% of the forecasts resulted in very good and good classifications, a significant figure. However, around 37% of the remaining forecasts were classified as regular and bad, representing a considerable percentage and focused the analysis on the relationship or link of each subtype with the classified forecast (Figure 5).

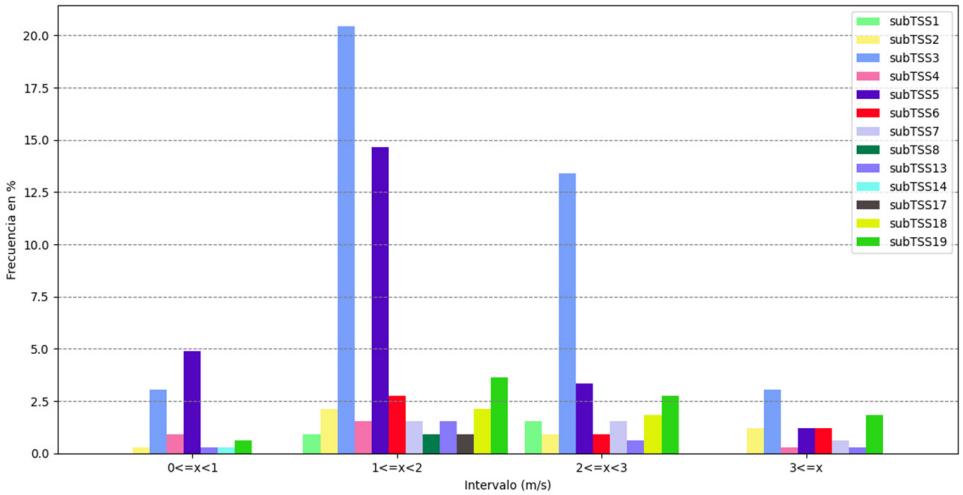

Figure 5. Frequency of the MAE statistic associated with the subTSS.

In general, it was noted that subtypes 3 and 5 were the most predominant and were present in all analyzed intervals. Of all the subTSS presented during the period, 8 (convergence and west troughs), 14 (Reversing cold front), and 17 (migratory continental anticyclone) did not show MAE values in the range of regular and bad. It was also found that subtypes 1 (subtropical anticyclone with first quadrant flow) and 18 (migratory anticyclone in the process of transformation) were never classified as bad by the MAE. This indicates that the SisPI had a good performance in representing these subTSS despite their low frequencies of occurrence.

3.3. Analysis of the Association between MAE and subTSS in the Rainy Period (RP) and Less Rainy Period (LRP)

3.3.1. Rainy Period (RP)

Figures 6 and 7 show the frequency distribution of MAE for the RP of May–October 2020. It presented a similar distribution to what was found for the annual case, with the good interval being the most frequent. Of the cases, 64.6% were classified as very good and good, while 35.4% were considered regular and bad.

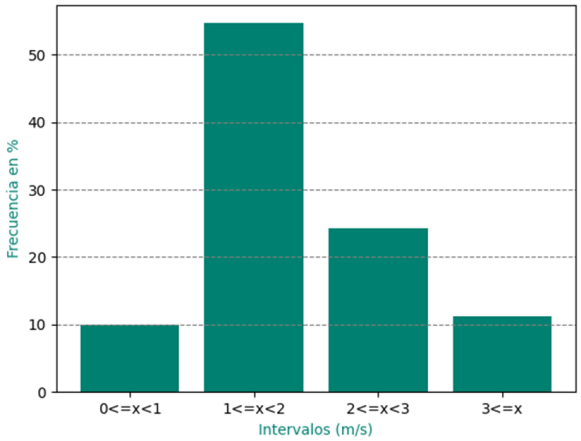

Figure 6. Frequency distribution of the MAE statistic for the rainy period (May–October 2020).

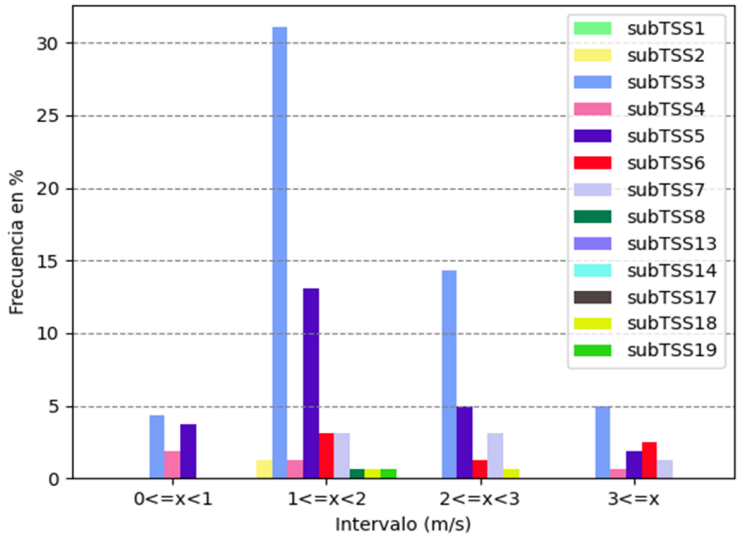

Figure 7. Behavior of the MAE statistic in the rainy period according to the subTSS (May–October 2020).

3.3.2. Less Rainy Period (LRP)

Figures 8 and 9 show the association between MAE and subTSS for the LRP, displaying a similar behavior to what has been analyzed so far. Once again, the intervals of very good and good encompassed the majority of cases, with 62.3%, while 37.7% represented the cases of regular and bad.

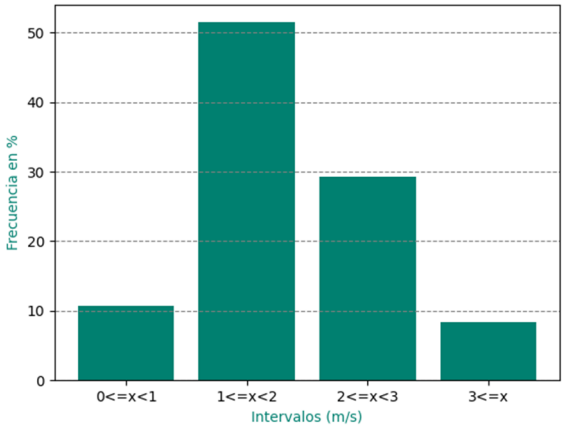

Figure 8. Frequency distribution of the MAE statistic for the less rainy period (November 2020–April 2021).

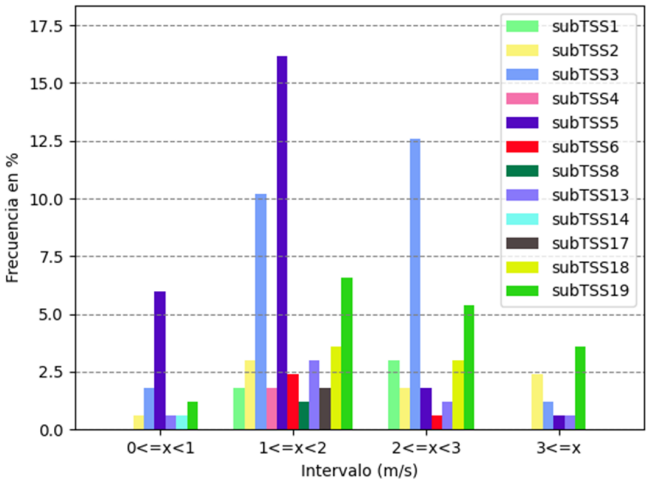

Figure 9. Behavior of the MAE in the less rainy period according to the subTSS (November 2020–April 2021).

3.4. Analysis of the Association between Regular and Bad MAE Values and subTSS in the Rainy Period (RP) and Less Rainy Period (LRP)

Considering that the cases classified as regular and bad represented around 37% of the entire sample studied, it was of interest to determine if there was any preferential relationship between the behavior of MAE and subtypes in either of the two seasonal periods for Cuba. The results for the RP and LRP are shown in Figure 10.

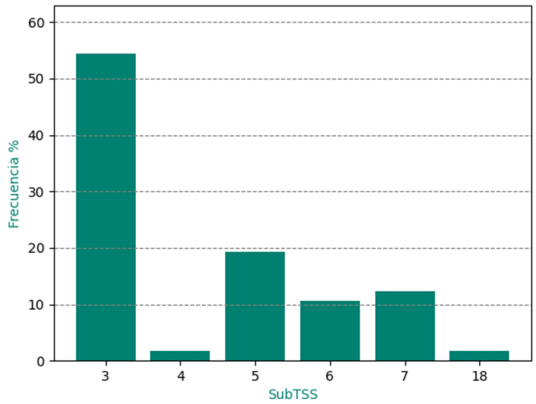

(**a**)

Figure 10. *Cont.*

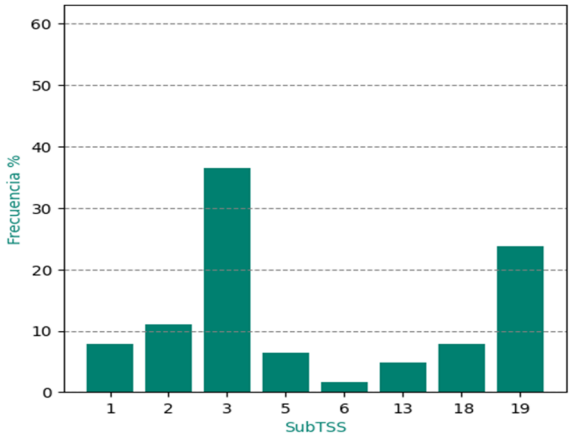

(**b**)

Figure 10. Frequency distribution of regular and bad MAE cases by subTSS for the rainy period (**a**) and the less rainy period (**b**).

3.4.1. RP Analysis

In Figure 10a, it can be observed that over 50% of the cases with an MAE between regular and bad corresponded to subtype 3; around 20% to subtype 5; approximately 12% to subtype 7; about 11% to subtype 6; and the rest with less than 5%. It was noteworthy that subtype 3 continued to have a high incidence of cases with an MAE index classified as regular and bad. This trend could be related to the lack of precision of SisPI in correctly predicting the position of the subtropical ridge, as pointed out by [26]. However, it is important to note that this statement requires further experiments to confirm it in the context of this study.

3.4.2. LRP Analysis

Despite the low frequency of subtype 19 in the study year, this subtype had a high percentage of cases where the wind speed forecast was classified as regular and bad according to the MAE, indicating that attention should be paid to this subtype by SisPI developers and weather forecasters in general.

3.5. Wind Speed Forecast Behavior during the Period May 2020–April 2021 via RMSE Analysis

Similar to the MAE analysis, it was decided to apply this classification of forecast error to analyze the root mean square error (RMSE).

Figure 11 illustrates the performance of the examined cases. A percentage greater than 42% of the forecasts were classified between very good and good, reflecting more favorable results. It is important to note, however, that 58% of the forecasts were classified as regular or bad, which motivated a more detailed analysis.

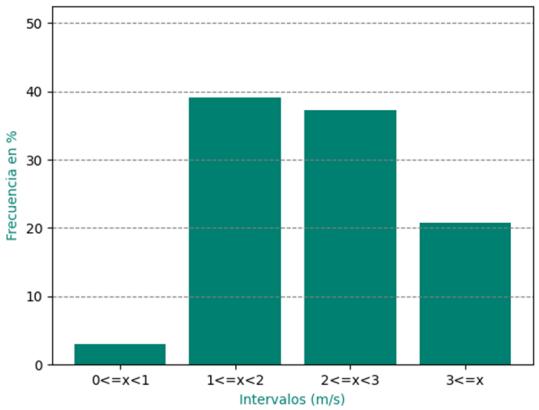

Figure 11. Frequency of the RMSE statistic.

The dynamics of RMSE in relation to the subTSS are shown explicitly in Figure 12. In general terms, subtypes 3 and 5 presented the highest prevalence.

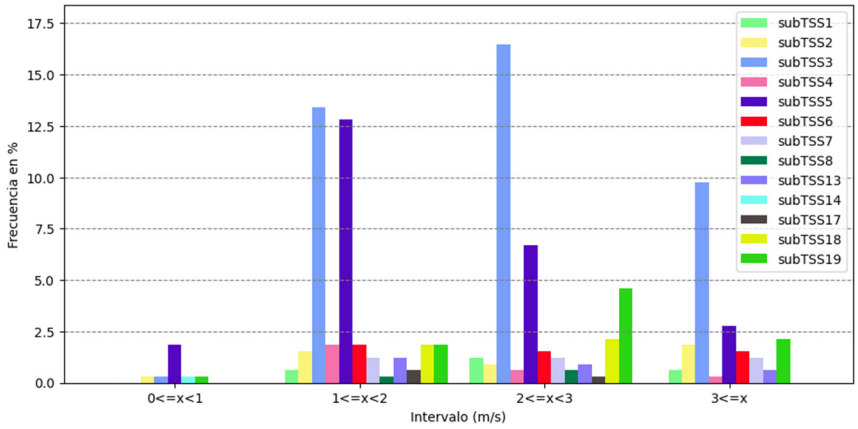

Figure 12. Frequency of the RMSE statistic associated with the subTSS.

3.6. Analysis of the Association between RMSE and subTSS in the Rainy Period (RP) and Dry Period (DP)

3.6.1. Rainy Period (RP)

Figures 13 and 14 show the frequency distribution of RMSE for the RP corresponding to the period May–October 2020. Of the cases, 40.4% were classified as very good and good, while 59.6% were considered as regular and bad.

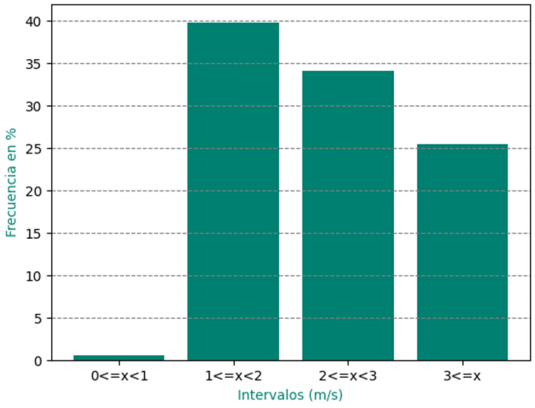

Figure 13. Frequency distribution of the RMSE statistic for the rainy period (May–October 2020).

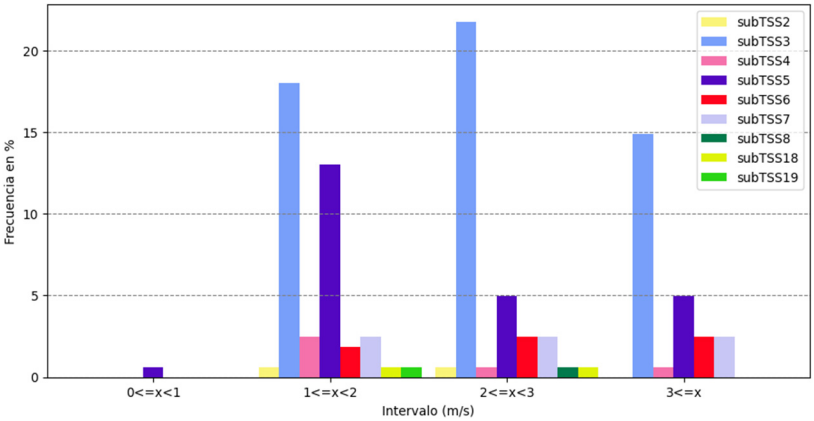

Figure 14. Frequency distribution of the RMSE statistic associated with the subtypes for the rainy period (May–October 2020).

3.6.2. Dry Period (DP)

Figures 15 and 16 show the relationship between RMSE and subtypes in the DP; 43.7% were considered very good and good, while 56.3% were categorized as regular and bad.

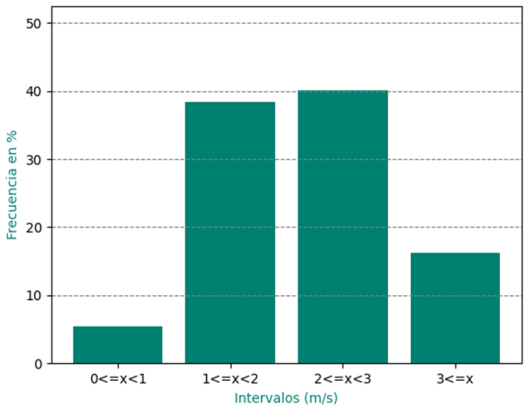

Figure 15. Frequency distribution of the RMSE statistic for the less rainy period.

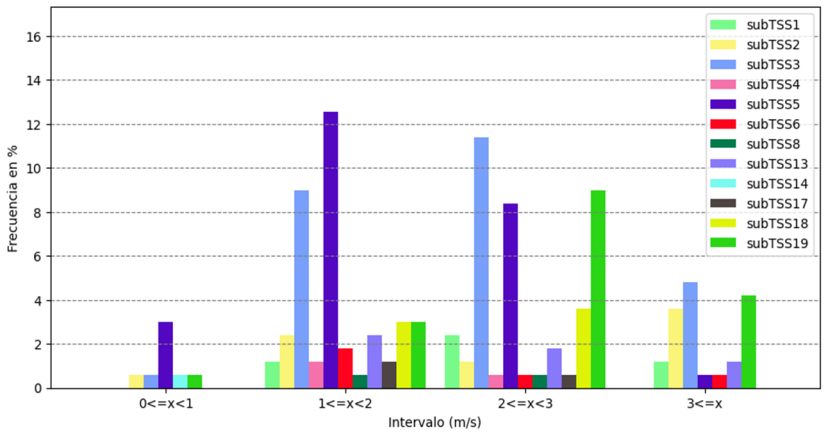

Figure 16. Behavior of the RMSE in the less rainy period according to the subTSS (November 2020–April 2021).

3.7. Analysis of the Association between Bad and Regular RMSE Values and subTSS in the Rainy Period (RP) and Dry Period (DP)

It is noteworthy that a high percentage of cases showed results between regular and bad, representing 58% of the analyzed sample. Therefore, it was considered necessary to further analyze these cases. Similar to the approach used in the MAE study, the analysis was carried out considering the two seasons of the year in Cuba, with the aim of evaluating if there was any correlation between the behavior of RMSE and subTSS during seasonal periods. The results during the rainy period (RP) and dry period (DP) are presented clearly in Figure 17.

3.7.1. Analysis of RP

Figure 17a shows that subtype 3 has a prevalence greater than 60%. While subtype 5 is evident with more than 15%. The remaining subtypes had less than 10% of the instances. Subtype 3, similar to the MAE analysis, concentrates the majority of cases with regular or bad RMSE, indicating a possible relationship with the tendency of SisPI to not correctly predict the position of the subtropical high, as indicated in the MAE observation.

3.7.2. Analysis of DP

When examining the behavior of RMSE for the cases of regular and bad in the DP (Figure 17b), it can be observed that although subtype 3 has decreased its frequency to less

than 30%, demonstrating a lower presence compared to RP, it still prevails among the cases of regular and bad classification. This suggests that subtype 3 is better represented by SisPI in this period of the year. However, the analysis highlights subtype 5 with around 15%.

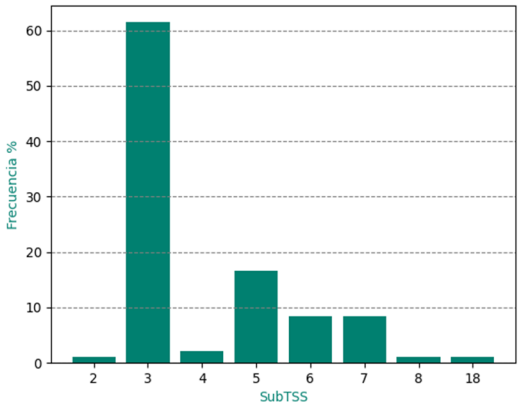

(**a**)

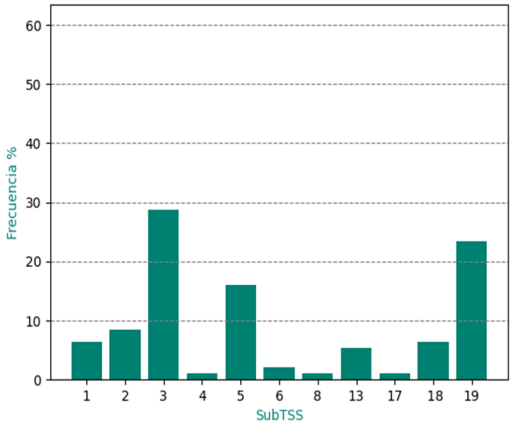

(**b**)

Figure 17. Frequency distribution of regular and bad RMSE cases by subTSS in the rainy period (**a**) and the less rainy period (**b**).

3.8. Behavior of Wind Speed Forecast in the Period from May 2020 to April 2021 via BIAS Analysis

The analysis of the BIAS statistic (Figure 18) allows us to see a general trend where an overestimation is observed in all hours.

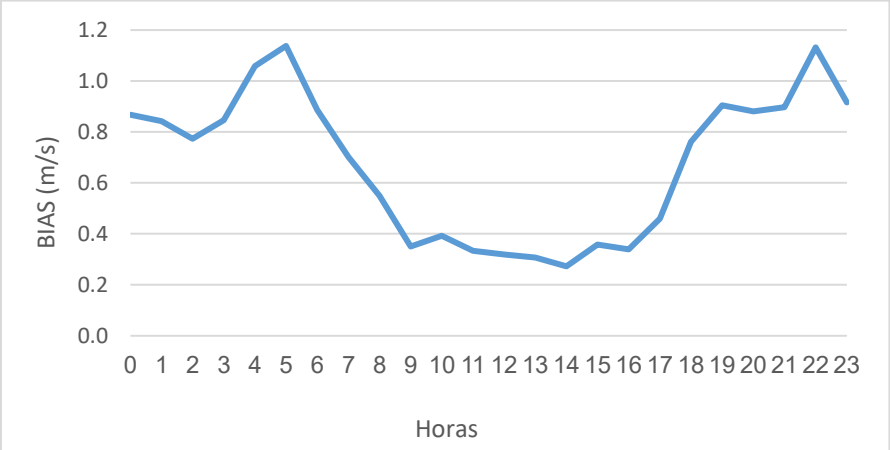

Figure 18. BIAS of wind speed.

It was evident that subtype 19, which represented more than 20% of the cases, had a significantly high frequency of wind speed forecasts classified as regular or bad despite its low frequency in the year of study, indicating that this subtype is poorly represented by SisPI and should receive more attention. The rest of the subtypes had frequencies below 10%.

The forecast overestimation was most noticeable during the early hours until 9 a.m. and then in the evening–night between 6 p.m. and 11 p.m., with a behavior between 0.3 m/s and 1.2 m/s. In the timeframe from 9 a.m. to 5 p.m., the behavior was more favorable, as it was closer to zero. This behavior turned out to be better compared to what was found by [18], whose BIAS values for PEGI and PEGII were underestimated in all timeframes, with a behavior between 0 m/s and −4 m/s.

3.9. Behavior of Wind Speed Forecast in the Period from May 2020 to April 2021 via R Analysis

Figure 19 shows the Pearson correlation coefficient R, the other analyzed statistic. It is easy to appreciate that there is a positive correlation, with values greater than 0.7 in the early morning hours until 9 am, from which the values begin to decrease to approximately 0.5 m/s at 5 p.m., after which they start to increase again up to 0.7 m/s.

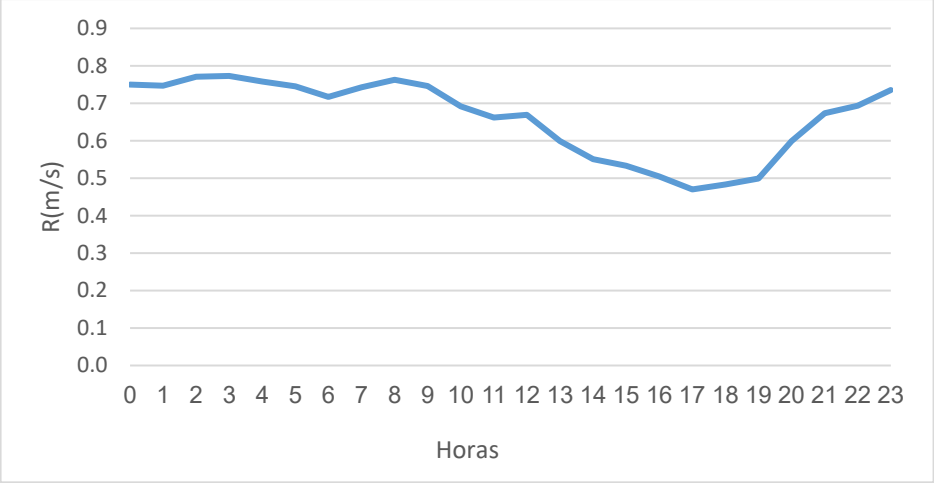

Figure 19. Pearson correlation coefficient between the values predicted by the model and the actual measurements.

4. Conclusions

The research conducted yielded the following conclusions:

- It was obtained that, in the case of MAE, 63.4% of the wind speed forecasts were classified as very good or good, while 36.6% were classified as regular and bad, which reflects the good representation of most subTSS by SisPI. However, for RMSE, it was obtained that 42% of the values fell between very good and good, and 58% of the forecasts were classified as regular and bad, which was not as favorable.
- The MAE analysis of the cases classified as regular and bad for both seasonal periods yielded well-defined results, highlighting subtype 3 (unperturbed extended anticyclonic flow), which represented over 50% of the cases in PLL and just over 35% in PPLL, reflecting the improvement by SisPI in forecasting this subtype in the low rainfall period. In the case of RMSE analysis, it was obtained that this subtype had a prevalence of over 60% in PLL and less than 35% in PPLL, showing a lower presence compared to PLL.
- Subtype 19 was the system that achieved the worst results, as despite its low frequency in the study year, over 50% of the days it was present, the wind speed forecast was classified as regular and bad.

- In the case of BIAS analysis, both parks showed favorable behavior, with overestimated values between 0 and 1.2 m/s. On the other hand, the R analysis also showed good behavior, between 0.4 and 0.8 m/s.

5. Recommendations

- Sharing the results of this research with SisPI developers, as well as with weather forecasters in general.
- Further investigating the relationship between TSS and forecast errors via new experiments.
- Incorporating the underlying subTSS into the wind speed forecast.

Author Contributions: Conceptualization, A.R.R.; methodology, D.M.P.A. and A.R.R.; software, D.M.P.A.; validation, D.M.P.A., A.R.R. and E.S.T.; formal analysis, D.M.P.A. and A.R.R.; investigation, D.M.P.A. and A.R.R.; resources, D.M.P.A., A.R.R. and E.S.T.; data curation, D.M.P.A.; writing—original draft preparation, D.M.P.A.; writing—review and editing, A.R.R., E.S.T., A.S.R., T.G.L. and R.O.B.; visualization, D.M.P.A., A.S.R., T.G.L. and R.O.B.; supervision, A.R.R. and E.S.T.; project administration, A.R.R. All authors have read and agreed to the published version of the manuscript.

Funding: This research was funded by the project "Improvement of the energy forecasting system for wind and photovoltaic parks connected to the National Electroenergy System".

Institutional Review Board Statement: Not applicable.

Informed Consent Statement: Not applicable.

Data Availability Statement: The data was provided by a government agency under a confidentiality agreement and its dissemination is not allowed at this time.

Conflicts of Interest: The authors declare no conflict of interest.

References

1. GWEC: Global Wind Energy Council. Global Wind Report. 2023. Available online: https://gwec.net/globalwindreport2023/ (accessed on 25 August 2023).
2. Ministerio de Energía y Minas de Cuba. Eólica. 2021. Available online: https://www.minem.gob.cu/es/actividades/energias-renovables-y-eficiencia-energetica/e%C3%B3lica (accessed on 25 August 2023).
3. Giebel, G.; Draxl, C.; Brownsword, R.; Kariniotakis, G.; Denhard, M. *The State-of-the-Art in Short-Term Prediction of Wind Power: A Literature Overview*, 2nd ed.; ANEMOS.plus: Oldenburg, Germany, 2011. [CrossRef]
4. Senkal, S.; Ozgonenel, O. Performance Analysis of Artificial and Wavelet Neural Networks for Short Term Wind Speed Prediction. In Proceedings of the 8th International Conference on Electrical and Electronics Engineering (ELECO), Bursa, Turkey, 28–30 November 2013. [CrossRef]
5. Sapronova, A.; Meissner, C.; Mana, M. Short-Time Ahead Wind Power Production Forecast. *J. Phys. Conf. Ser.* **2016**, *749*, 012006. [CrossRef]
6. Li, Q.; Hammerschmidt, C.; Pellegrino, G.; Verwer, S. Short-term Time Series Forecasting with Regression Automata. In Proceedings of the KDD '16, San Francisco, CA, USA, 13–17 August 2016.
7. Xie, A.; Yang, H.; Chen, J.; Sheng, L.; Zhang, Q. A short-term wind speed forecasting model based on a multi-variable long short-term memory network. *Atmosphere* **2021**, *12*, 651. [CrossRef]
8. Li, Z.; Luo, X.; Liu, M.; Cao, X.; Du, S.; Sun, H. Short-term prediction of the power of a new wind turbine based on IAO-LSTM. *Energy Rep.* **2022**, *8*, 9025–9037. [CrossRef]
9. Lv, S.; Wang, L.; Wang, S. A Hybrid Neural Network Model for Short-Term Wind Speed Forecasting. *Energies* **2023**, *16*, 1841. [CrossRef]
10. Saini, V.K.; Kumar, R.; Al-Sumaiti, A.S.; Sujil, A.; Heydarian-Forushani, E. Learning based short-term wind speed forecasting models for smart grid applications: An extensive review and case study. *Electr. Power Syst. Res.* **2023**, *222*, 109502. [CrossRef]
11. Wang, X.; Li, J.; Shao, L.; Liu, H.; Ren, L.; Zhu, L. Short-Term Wind Power Prediction by an Extreme Learning Machine Based on an Improved Hunter–Prey Optimization Algorithm. *Sustainability* **2023**, *15*, 991. [CrossRef]
12. Roque, A.; Borrajero, I.; Hernández, A.; Sierra, M. Short-Term Energy Forecast for the Gibara I and Los Canarreos Wind Farms. In *Technical Report*; P211LH003–004; Instituto de Meteorología de Cuba: Havana, Cuba, 2015.
13. Roque, A.; Sierra, M.; Borrajero, I.; Ferrer, A. Short-Term Wind Forecast in Meteorological Reference Towers for the Cuban Wind Program. In *Technical Report*; Instituto de Meteorología de Cuba: Havana, Cuba, 2015.
14. Roque, A.; Hernández, A.; Borrajero, I.; Sierra, M.; Valdéz, A. Pronóstico de viento a corto plazo utilizando el modelo WRF en tres regiones de interés para el Programa Eólico Cubano. *Rev. Cuba. Meteorol.* **2016**, *22*, 164–187.

15. Martínez, B.; Roque, A. Pronóstico energético a muy corto plazo para el Parque Eólico Gibara I utilizando un modelo autorregresivo. *Rev. Cuba. Meteorol.* **2019**, *25*, 168–178.
16. Fuentes, A.; Sierra, M.; Roque, A. LSTM Model for Wind Speed and Power Generation Nowcasting. *Environ. Sci. Proc.* **2022**, *13*, 30.
17. Sierra, M.; Fuentes, A.; Roque, A.; Rosquete, A.; Patiño, D. Comparación del pronóstico de Viento Qenerado por el Modelo WRF y dos Modelos LSTM. *Rev. Cuba. Meteorol.* **2023**. Available online: https://cu-id.com/2377/v29n3e04 (accessed on 25 August 2023).
18. Roque, A.; Ferrer, A.; Sierra, M.; Borrajero, I. Pronóstico numérico a corto plazo de la rapidez del viento para los parques eólicos de Gibara I y II. *Rev. Cuba. Meteorol.* **2022**, *28*, 4–6.
19. Patiño, D.; Roque, A.; Soler, E. EMA del pronóstico a corto plazo de la rapidez del viento para el parque eólico Gibara I según el TSS influyente. *Rev. Cuba. Meteorol.* **2023**, *29*, 3–8.
20. Soler, E.; Lecha, L.; Sánchez, L.; Naranjo, Y. *Catálogo de los Tipos de Situaciones Sinópticas que Influyen Sobre Cuba*; Centro Meteorológico de la Isla de la Juventud: Nueva Gerona, Cuba, 2020. [CrossRef]
21. Sierra, M.; Borrajero, I.; Ferrer, A.; Morfá, Y.; Morejón, Y.; Hinojosa, M. *Estudios de Sensibilidad del SisPI a Cambios de la PBL, la Cantidad de Niveles Verticales y, las Parametrizaciones de Microfísica y Cúmulos, a Muy Alta Resolución*; Informe de Resultado Instituto de Meteorlogía: La Habana, Cuba, 2017. Available online: https://www.researchgate.net/publication/ (accessed on 18 May 2023).
22. Carrasco, M.; Roque, A.; Sánchez, O. Local Breeze Effects on the Wind Energy Generation in the Northern Coast of Cuba. *Wind. Eng.* **2011**, *35*, 635–648. [CrossRef]
23. Roque, A.; Carrasco, M.; Reyes, P. Características del perfil vertical del viento en la capa superficial atmosférica sobre Cuba, atendiendo a la estratificación térmica de la atmósfera. *Cienc. Tierra Espac.* **2015**, *16*, 189–200.
24. Martínez, B.; Roque, A. Disminución de la rapidez del viento en la capa superficial atmosférica. Su influencia en el aprovechamiento eólico. *Rev. Cuba. Meteorol.* **2015**, *21*, 49–61.
25. Perdigón, J.; Rodríguez, G. Condiciones Sinópticas más Favorables Para el Aprovechamiento de la Energía Eólica en Cuba. Período Poco Lluvioso. *Rev. Cuba. Meteorol.* **2012**. Available online: http://rcm.insmet.cu/index.php/rcm/article/view/19 (accessed on 25 August 2023).
26. Paula, J.; Sierra, M.; González, P. Analysis of SisPI Performance to Represent the North Atlantic Subtropical Anticyclone. *Environ. Sci. Proc.* **2022**, *19*, 40. [CrossRef]